Materials Today Energy 49 (2025) 101821

Contents lists available at ScienceDirect

Materials Today Energy

journal homepage: www.journals.elsevier.com/materials-today-energy/

Exploring the diversity of molecular carbon oxides, and their potential as high energy density materials

Elizaveta E. Vaneeva [a,*], Sergey V. Lepeshkin [a,b], Dmitry V. Rybkovskiy [a], Artem R. Oganov [a]

[a] Skolkovo Institute of Science and Technology, Bolshoy Boulevard 30, bld. 1, 121205, Moscow, Russian Federation
[b] Lebedev Physical Institute, Russian Academy of Sciences, Leninsky Ave. 53, 119991, Moscow, Russian Federation

A B S T R A C T

We have conducted a systematic structure prediction of C_nO_m molecules across a wide compositional range ($0 \leq n, m \leq 16$) using the first-principles evolutionary global optimization algorithm USPEX. Results show a diverse range of structural patterns which vary with molecular size and O/C ratio. Stability of C_nO_m molecules was explored using approaches borrowed from nanocluster studies, where stability with respect to an ensemble of neighboring compositions is used as a criterion of "magic" (particularly preferable) clusters. In addition, we have identified molecules that are both magic and release a high amount of energy during their decomposition, and found that the most promising molecules have compositions in or near the range $1 \leq O/C \leq 2$. Our findings give clues for future syntheses and explorations of oxocarbons and suggest them as a new promising class of high energy density materials.

1. Introduction

Carbon oxides (oxocarbons) are compounds composed solely of carbon and oxygen atoms. When people think about carbon oxides, they usually remember the simplest CO and CO_2 molecules, however that only scratches the surface. Many other carbon oxides also exist, for example, mellitic anhydride ($C_{12}O_9$) has been known for two centuries and can be synthesized relatively easily. As another example, C_3O_2 is made by dehydrating malonic acid ($C_3H_4O_4$), by electric discharge in CO gas, or by heating gas. Oxocarbons are promising for many applications including advanced energetics, electrode materials for Li-ion batteries, atmospheric chemistry, and biochemical studies [1–4]. Carbon monoxide is abundant in various astronomical environments, including the interstellar medium, comets, planets, and even metal-poor galaxies [5]. Also, oxocarbons may be present on white dwarfs as remnants of carbon burning [6]. This widespread presence suggests the potential existence of polymeric forms of C-O compounds in planets, making it a target of astrophysical research [1]. Additionally, carbon oxides play a significant role when examining the combustion products of common hydrocarbon fuels such as kerosene, ethanol and dimethyl ether.

CO and N_2 molecules are isoelectronic, and the strength of the CO triple bond (11.16 eV) [7] even surpasses that of the N_2 (9.79 eV) [7]. Polymeric forms of nitrogen [8–10] at high pressure and metal polynitrides [11–14], containing simple N-N or double N=N bonds, have been suggested as high energy density materials (HEDMs) due to highly exothermic decomposition into molecular nitrogen with triple $N \equiv N$ bond. The rationale here is that the triple $N \equiv N$ bond is much stronger that three single N-N bonds (9.79 eV vs. 3*1.73 = 5.19 eV) [7]. In C_nO_m molecules things are slightly different: the energy of a double C=O bond (8.28 eV) [7] is much better than that of two single C-O bonds (2*3.71 = 7.42 eV [7]), and triple $C \equiv O$ bond is similar to 3 times the energy of single bond. As a consequence, decomposition of singly-bonded C_nO_m molecules into those with double C=O bonds is expected to release much energy, which creates the possibility to use oxocarbons as HEDMs. Polymerized carbon monoxide is also considered a potential HEDMs, in close analogy with polymeric nitrogen, prompting investigations into various polymeric forms of CO, their crystal structures, and energetics at high pressures [15,16]. In recent years, research on carbon oxides as HEDMs has primarily focused on small or stoichiometric compounds. Studies have examined the detonation velocities and pressures of various oligomers and co-oligomers of CO and CO_2, as well as their decomposition reactions, identifying C_2O_4 as a promising candidate [17]. Also, non-planar oxocarbons C_2O_2 and C_4O_4 are structurally similar to nitrogen molecules, but only decomposition paths releasing CO molecules were studied, not considering CO, CO_2, C_2, O_2 [18]. Some larger C-O molecules have been also evaluated for their potential as HEDMs. Cyclic $(CO)_n(CO_2)_m$ co-oligomers, such as C_2O_3, C_3O_5, and C_4O_6, and their decomposition into CO, CO_2, and O_2 have been analyzed [19]; notably, C_4O_6 has been synthesized experimentally [20]. Also, carbon oxides CO_m ($m > 2$) with high oxygen content are highly energetic too

* Corresponding author.
E-mail address: Elizaveta.Vaneeva@skoltech.ru (E.E. Vaneeva).

https://doi.org/10.1016/j.mtener.2025.101821
Received 15 November 2024; Received in revised form 16 January 2025; Accepted 27 January 2025
Available online 6 February 2025

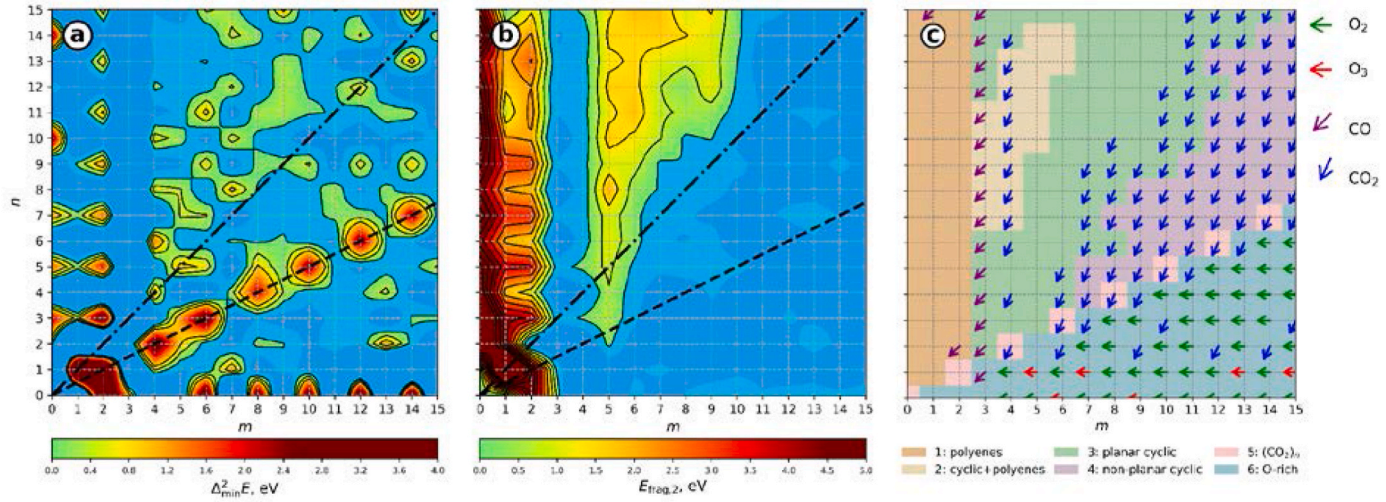

Fig. 1. Interpolated heat maps: (a) Δ^2_{min} and (b) $E_{frag,2}$ (in eV) of C_nO_m molecules as a function of n and m. Regions of instability are marked in blue. Dashed lines are molecules corresponding to compositions with stoichiometry O/C equal to 1 and 2. (c) Classification scheme of C_nO_m molecules. The composition space is divided into 6 classes according to structural features and bonding character. This scheme also illustrates the composition changes of molecules during fragmentation. For each point (n, m) an arrow is drawn pointing towards the largest fragment obtained during the fission of the C_nO_m molecule, if it is energetically preferable. Arrows are colored depending on the type of the smallest fragment (O_2, O_3, CO and CO_2).

[1].

Another subject of interest is $(CO)_n$ compounds due to their application in Li-ion batteries (LIBs). Cyclic $(CO)_n$ molecules (where $n = 4, 5, 6$) with multiple electron-withdrawing C=O groups exhibit promising potential as cathode materials in LIBs owing to their redox-active nature [4,21]. Devices, containing Li as anode, quasi-solid electrolyte and C_5O_5 as the cathode material exhibit in experiment exceptional electrochemical performance compared to other reported organic carbonyl electrode materials for LIBs.

Despite the increased interest in carbon oxides, their structure determination has been conducted to date only for small areas of composition space or stoichiometric compounds. The atomic structures of C_nO_m molecules are also available in the databases of biomolecules. However, they do not contain data for all compositions, for example, in the Pubchem [22] database for the compositional region $1 \le n, m \le 15$ (225 different formulas) there are data only for 78 formulas, and there is no certainty that the provided molecules are real ground states.

In this work, we conducted an extensive systematic study of C_nO_m molecules, covering a wide compositional range ($0 \le n, m \le 16$). We utilize global optimization methods in conjunction with density functional theory (DFT) calculations to determine ground-state structures as well as low-energy isomers. We studied their geometric and energetic characteristics and identified the most favorable ("magic") molecules. Additionally, we calculated the energy output of decomposition processes and identified compounds which may be promising HEDMs.

2. Computational methodology

Structures of C_nO_m molecules were identified using the evolutionary variable-composition global optimization algorithm for molecules and nanoclusters. This algorithm, developed by our group and implemented in the USPEX code [23,24], leverages the exchange of structural fragments between molecules of different compositions, demonstrating up to 50-fold acceleration compared to conventional techniques that performs structure search for each composition separately [25].

To ensure reliable and accurate structure prediction, the calculation procedure involved several steps. Initially, the USPEX search was conducted using the evolutionary algorithm in conjunction with the *ab initio* VASP code [26,27], which employs the projector-augmented wave method [28] and the Perdew–Burke–Ernzerhof (PBE) exchange-correlation functional [29]. Spin polarization was taken into account in these calculations.

Then, 25 lowest-energy isomers from each composition were selected for further refinement using the GAUSSIAN code, applying the B3LYP hybrid functional and the 6-311G+(d,p) basis set [30]. For these molecules, we checked various spin states and identified the lowest-energy one. We calculated vibrational spectra of all these structures and verified that they have no imaginary frequencies. For each ground state structure we calculated its Gibbs free energy at T = 300 K.

3. Structure and stability of C_nO_m molecules

Ground-state structures of C_nO_m molecules were found in a vast compositional area of $0 \le n, m \le 16$, which contains 288 different compositions. Pure carbon molecules were studied in depth by many researchers, including our group [31,32]. O_m molecules were investigated only up to $m = 8$ [33], when $m > 8$ oxygen rings decompose into a number of O_2 molecules. Comparing our results in range $1 \le n, m \le 15$ with the PubChem database, we found that for 40 C_nO_m compositions we identified the same global minima. For 38 compositions, we discovered lower-energy structures, and to the best of our knowledge, 147 molecular compositions were never studied before (see ESI Table S1). It should be noted that all C_nO_m ground-state structures are singlets, except C_2, C_4, C_6, C_8, C_{13}, C_nO ($n = 2, 4, 6, 8, 10, 12$), C_nO_2 ($n = 2, 4, 6, 8, 10, 12, 14, 16$), O_2 and O_3, which are triplets. The *xyz* coordinates of all calculated ground-state structures are provided in ESI Section S2.

Regarding stability of C_nO_m molecules, we can formulate criteria elaborated in our previous studies [25,31,32,34–37], based on their ground-state energies $E(n, m)$. In the first criterion, we consider stability with respect to the exchange of one carbon or one oxygen atom between two identical molecules C_nO_m. The energy change can be written as:

$$\Delta^2_C E(n,m) = E(n+1,m) + E(n-1,m) - 2E(n,m), \quad (1a)$$

$$\Delta^2_O E(n,m) = E(n,m+1) + E(n,m-1) - 2E(n,m). \quad (1b)$$

Then, we characterize the degree of stability of the molecule by the minimum of these values: $\Delta^2_{min} = \min\{\Delta^2_C E, \Delta^2_O E\}$. Molecules with a positive Δ^2_{min} are referred to as "magic", drawing an analogy to magic clusters in nanoscience and magic nuclei in nuclear physics. It is observed that magic nanoclusters are more abundant than others [25, 34–39]. In our previous studies it was also shown that this criterion equally is applicable to organic molecules: it can predict their

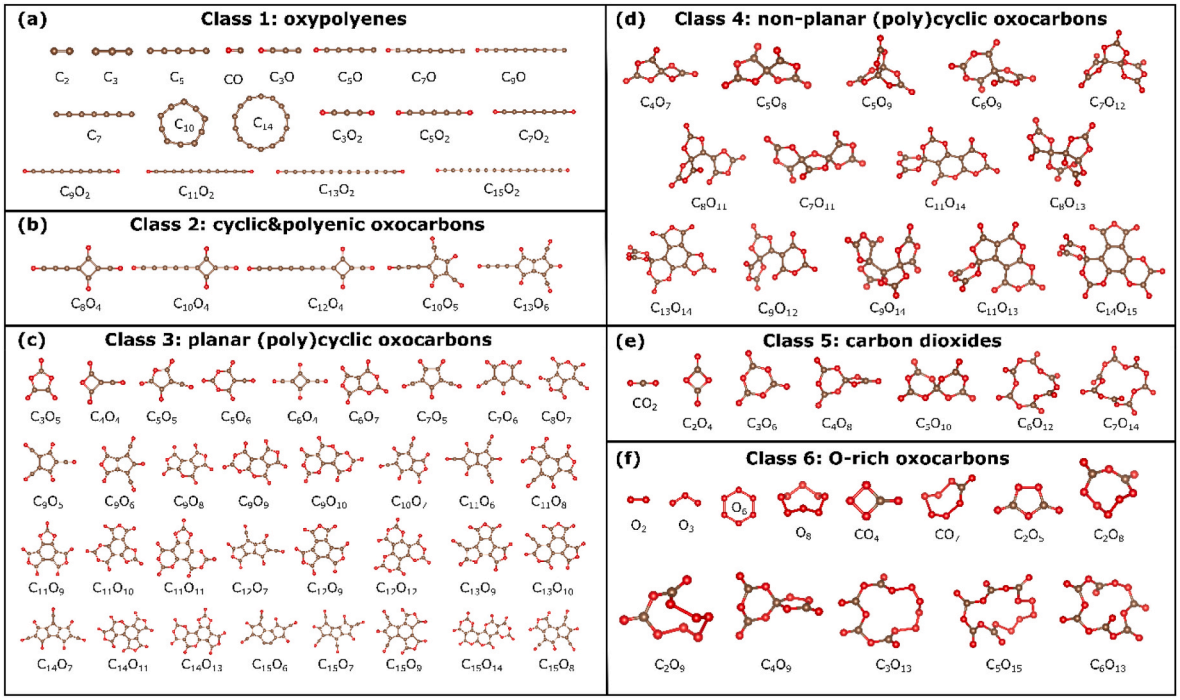

Fig. 2. C_nO_m molecules with $\Delta^2_{min} > 0$ from classes 1–6, classified by their structural topology. Brown spheres are carbon atoms and red ones are oxygen atoms, respectively.

abundance in various environments (interstellar medium, planetary atmospheres and crude oil) and ease of synthesis [31,32]. This can be explained as follows: if two molecules with $\Delta^2_{min} < 0$ collide it is energetically favorable for them to exchange one atom, therefore, the concentration of such molecules will gradually decrease, in favor of molecules with $\Delta^2_{min} > 0$.

The values of $\Delta^2_{min}(n, m)$ for binary molecules can be conveniently visualized as a 2-dimensional heatmap. Fig. 1a shows an interpolated map of $\Delta^2_{min}(n, m)$ for C_nO_m molecules with n, m up to 15. Red color indicates highly stable magic molecules, blue color represents unstable compositions ($\Delta^2_{min} < 0$). Light blue regions indicate molecules with moderately negative Δ^2_{min} ($-0.4\ \text{eV} \le \Delta^2_{min} \le 0$). Looking at the map, one can immediately see that the most fundamental molecules such as carbon monoxide (CO), carbon dioxide (CO_2), oxygen molecule (O_2) indeed have the greatest stability (red color in Fig. 1a). In general, magic compositions form islands and ridges of stability, scattered throughout the map, and will be discussed below.

Another stability criterion characterizes resistance to fragmentation. Here we identify molecules that can spontaneously decompose. To this end, we consider all possible channels of fragmentation of a given molecule for the decomposition into two fragments:

$$C_nO_m \rightarrow C_aO_b + C_{n-a}O_{m-b}, \text{where } 0 \le a \le m, 0 \le b \le n \quad (2)$$

The fragmentation energy of each reaction is found as:

$$E_{frag,2}(n, m, a, b) = E(a, b) + E(n - a, m - b) - E(n, m). \quad (3)$$

We are looking for the decomposition into the most stable fragments, hence, we calculated the minimal value of all fragmentation energies:

$$E_{frag,2}(n, m) = \min_{a,b} E_{frag,2}(n, m, a, b). \quad (4)$$

The interpolated heatmap of fragmentation energy $E_{frag,2}(n, m)$ is shown on Fig. 1b. We see two big regions with positive values of $E_{frag,2}$: C_nO_m molecules ($m \sim 0$–2) with the highest values of $E_{frag,2}$ and a Manhattan-shaped region between $m = 4$ and $m = 10$. The most resistant to decomposition are CO, CO_2 and O_2 molecules, as well as pure carbon clusters. Blue sea contains C_nO_m molecules that could decompose easily, thus, will be investigated further as HEDMs. Fig. 1c illustrates a scheme where the compositional areas corresponding to each class are highlighted in different colors. Additionally, it visually summarizes molecular fission of unstable compositions (where $E_{frag,2} > 0$): it is represented by an arrow pointing toward the largest fragment obtained during fission. The color of each arrow indicates the smaller fragment of fission: O_2, O_3, CO, CO_2.

Additionally, we have used a third criterion, the HOMO−LUMO gap. Fig. S1 (ESI, Section 1) shows interpolated heatmaps of gaps for C_nO_m molecules. This gap is a key factor in determining molecule's electronic properties, such as its electronic polarisability (and, hence, reactivity), and optical characteristics. Molecules with a wide HOMO-LUMO gap are typically more stable and less reactive.

The obtained ground-state structures of C_nO_m molecules reveal a wide variety of structural patterns, depending on stoichiometry and molecule size. For further analysis we divided all C_nO_m molecules into 6 classes according to structural features and bonding character: (1) and (2) pure carbon molecules and molecules with polyenic bonds; (3) and (4) cyclic molecules with C-C, C=C, C-O and C=O bonds; (5) molecules with only C-O bonds; (6) molecules with peroxy-bonds (-O-O-) and pure oxygen molecules. Magic representatives of each class are drawn in Fig. 2 and will be discussed below.

The 1st class contains C_nO_m molecules (where $0 \le m \le 2$), including pure carbon molecules and molecules containing 1 or 2 oxygen atoms (Fig. 1a). C_2, C_3, C_5, and C_7 are linear chains and C_{10}, C_{14} are rings, which agrees with previous studies [40]. C_nO and C_nO_2 molecules are linear carbon oxides with one or two terminal oxygen atoms. C_mO_2 oxides, being cumulenes, following the general formula $O{=}(C{=})_nO$, are observed in nature. Among them are metastable carbon suboxide C_3O_2 and pentacarbon dioxide C_5O_2, which is stable in solution [41,42]. Some carbon oxides were detected in the interstellar medium: dicarbon monoxide C_2O [43], tricarbon monoxide C_3O [44].

The 2nd class comprises molecules featuring cyclic carbon-containing fragments with polyenic substituents terminated by a carbonyl group (Fig. 2b). These molecules typically consist of 3- or 4-membered rings with several carbonyl C=O fragments and one long-chained functional group. The entire π-system of these molecules

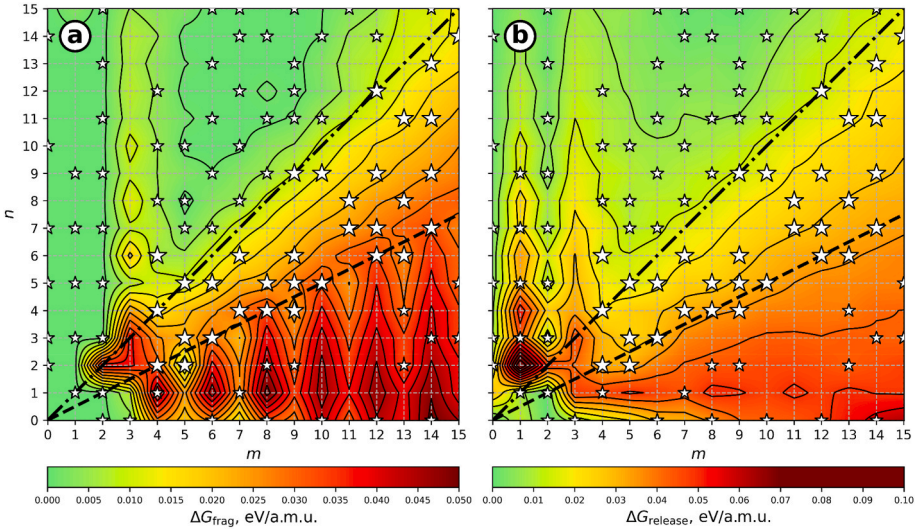

Fig. 3. Interpolated heatmaps showing (a) ΔG_{frag} - energy release in fragmentation reactions into the most favorable set of smaller molecules and (b) $\Delta G_{release}$ height above the convex hull, where G is the Gibbs free energy of each cluster calculated at 300 K. Dashed and dot-dashed lines show O/C ratios equal to 1 and 2, respectively. Stars denote magic molecules ($\Delta^2_{min} > 0$), larger stars indicate magic molecules promising as HEDMs.

allows for electron delocalization, which stabilizes the structure by lowering its overall energy. Resonance structures of these molecules exhibit conjugated polyynic chains with sp-hybridized carbon atoms.

The 3rd class are planar oxocarbons with (poly)cyclic structure (Fig. 3c). It includes molecules C_nO_m with $m \geq 3$ and $m/n \leq 1$, excluding those belonging to 2nd class. Oxocarbons from this class possess the highest values of the HOMO-LUMO gap (see Fig. S1, ESI). This class contains anhydrides and oxalates, among which are, for example, mellitic anhydride ($C_{12}O_9$) and dioxane tetraketone (C_4O_6) [20]. Dioxane tetraketone (C_4O_6) can be synthesized by reacting oxalyl chloride ($C_2O_2Cl_2$) with silver oxalate ($Ag_2C_2O_4$) at low temperature and pressure under an inert atmosphere. Mellitic anhydride was obtained as a derivative of the corresponding acid from mineral mellite by *Friedrich Wöhler* [45,46] and dioxane tetraketone obtained in solution of diethyl ether [20].

Molecules with stoichiometry O/C = 1 ($(CO)_n$ and $n \leq 12$) form the 3rd class of molecules. This stoichiometric group is one of the most studied theoretically [47]. Previously, it was assumed that $(CO)_m$ ground-state molecules have cyclic structures with carbonyl groups. On the contrary, we have discovered that ground-state structures of these molecules do not have a single topological pattern. C_2O_2 has a triplet ground state, whereas all other molecules of this class are in the singlet ground state.

We assign non-planar (poly)cyclic molecules to a distinct 4th class (Fig. 2d). This class comprises relatively large C_nO_m ($m \geq 7$) molecules, which generally fall between $(CO)_n$ and $(CO_2)_n$. What sets this class apart from the 3rd one is the presence of cycles sharing a common carbon atom, with the exception of the condensed rings found in the C_5O_9 molecule. Additionally, molecules of this class do not contain carbonyl C=O fragments as functional groups of cycles.

$(CO_2)_n$ ($n \leq 7$) molecules comprise the 5th class (Fig. 2e). Its main distinction from the previous classes is the absence of C-C bonds. Oligomers of CO_2 have only carbonyl C=O bond and ether C-O-C bonds. They exhibit structural similarity, with all molecules beginning with C_2O_4 units constructed from -O-C(=O)- building blocks. Our predicted ground-state structures of small $(CO_2)_n$ (n = 2, 3) are consistent with structures discussed lately [48]. As the value of n increases, molecules with 4-membered rings are found, followed by 6-membered rings and larger rings. $(CO_2)_n$ molecules have the highest values of Δ^2_{min}, which speaks of their synthetic possibility (Fig. 1a). This has been experimentally confirmed; for instance, C_3O_6 has been synthesized [49].

The 6th class contains oxygen-rich C_nO_m molecules and pure oxygen molecules O_m. These molecules have O/C > 2 (Fig. 2f) and have O-O bonds. Cyclic oxygen-rich CO_m (m = 3–8) molecules were extensively studied theoretically by *Kaiser and Mebel* [1]. They discovered that for molecules with $m \geq 5$ it is more favorable to form one cycle rather than 2 fused cycles, which agrees with our results. CO_3, CO_4, CO_5 [50], CO_6 [51] exist in low-temperature matrices of CO_2 ices. As for pure oxygen molecules, besides O_2 and O_3 we obtained several closed-ring O_n molecules, e.g., hexaoxygen O_6 and octaoxygen O_8; they are structurally similar to S_6 and S_8 [33], respectively. Structures and stability of S_n molecules were recently studied in our group [36].

The examples provided above demonstrate that the magicity criterion (Δ^2_{min}) can provide insight into the chemical synthesis of C_nO_m molecules. Molecules with a positive Δ^2_{min} value are easier to synthesize and more frequently observed across various environments.

4. HEDMs basing on C_nO_m molecules

This section is focused on studying the potential of using C_nO_m molecules as high energy density materials. Knowledge of the energies of molecules in the whole compositional area allows one to estimate the energy released during the decomposition of each molecule. Further we will consider several different processes - (1) decomposition into an arbitrary number of fragments and (2) rough approximation of decomposition of the corresponding molecular crystal into more stable compounds. To get closer to real conditions, we considered the process at 300 K, so, instead of the internal energy taking the Gibbs free energy.

(1) First, we calculate the maximum energy that can be obtained from a given molecule by breaking it down into smaller fragments. So, we consider decomposition into an arbitrary number (k) of fragments:

$$C_nO_m \rightarrow C_{x1}O_{y1} + C_{x2}O_{y2} + \ldots + C_{xk}O_{yk}, \quad (5)$$

where expressions $x_1 + x_2 + \ldots + x_k = n$ and $y_1 + y_2 + \ldots + y_k = m$ should be satisfied. The energy of this reaction, normalized by the molar mass of original molecule, is:

Table 1
The most promising high energy density C_nO_m molecules uncovered in our study (enumerated, their structures are shown in the right part of the table), given together with their caloricity, $\Delta G_{release}$. $\Delta G_{release}$ is given in MJ/kg for comparison of the heat of explosion of TNT (4.2 MJ/kg).

N⁰	Molecule	$\Delta G_{release}$ (MJ/kg)	$\frac{\Delta G_{release}\ (C_nO_m)}{\Delta G_{release}\ (TNT)}$	
1	C_4O_9	3.4	0.81	(1)C_4O_9 (2)C_4O_8 (3)C_6O_{13}
2	C_4O_8	3.3	0.78	
3	C_6O_{13}	3.3	0.77	
4	C_6O_{12}	3.2	0.75	
5	C_5O_{10}	3.1	0.74	
6	C_7O_{14}	3.1	0.73	(4)C_6O_{12} (5)C_5O_{10} (6)C_7O_{14}
7	C_2O_5	3.0	0.72	
8	C_2O_4	3.0	0.71	
9	C_4O_7	2.9	0.69	
10	C_7O_{12}	2.8	0.67	
11	C_5O_9	2.8	0.66	(7)C_2O_5 (8)C_2O_4 (9)C_4O_7
12	C_8O_{13}	2.7	0.65	
13	C_3O_6	2.7	0.65	
14	C_7O_{11}	2.6	0.62	(10)C_7O_{12} (11)C_5O_9 (12)C_8O_{13}
15	C_9O_{14}	2.6	0.61	
				(13)C_3O_6 (14)C_7O_{11} (15)C_9O_{14}

$$\Delta G_{frag}(m,n,k,x_1,\ldots,x_{k-1},y_1,\ldots,y_{k-1}) = 1 \,/\, M(C_nO_m)^*(G(m,n) - G(x_1,y_1) - \ldots - G(x_k,y_k)), \quad (6)$$

where $M(C_nO_m)$ is the molar mass of the C_nO_m molecule and G is Gibbs free energy. We are looking for the decomposition into such fragments that the released energy be minimal:

$$\Delta G_{frag}(m,n) = \min_{k,x1,\ldots,xk-1,y1,\ldots,yk-1} \Delta G_{frag}(m,n,k,x_1,\ldots,x_{k-1},y_1,\ldots,y_{k-1}). \quad (7)$$

The value of ΔG_{frag} essentially shows how much energy can be obtained from a given compound per unit mass. The higher this value, the more promising the molecule is as a HEDM. Fig. 3a displays the interpolated heat map of $\Delta G_{frag}(m, n)$. The pattern of the ΔG_{frag} roughly coincides with the pattern of $E_{frag,2}$, taken with the opposite sign: the values of ΔG_{frag} are higher for molecules with $m = 3$–4 or with O/C ≥ 1, and the greater O/C, the greater the value of ΔG_{frag}. The highest values of ΔG_{frag} are reached for molecules with O/C > 2 or belonging to a small island consisting of 3 molecules (C_2O_2, C_2O_3 and C_3O_3). However, molecules with an O/C > 2 contain excess oxygen, which tends to easily detach as O_2 molecules. The molecules C_2O_2, C_2O_3, C_3O_3 are not magic, so their synthesis may face difficulties. Thus, the compositional region between and including lines $1 \leq$ O/C ≤ 2 corresponds to the molecules that have the potential to be experimentally obtained and have reasonably high ΔG_{frag}.

(2) Secondly, we want to find roughly how much energy is released during the decomposition of a molecular crystal, consisting of corresponding molecules, into the most stable compounds. For this purpose for each compound C_nO_m we calculate the energy of formation using the formula:

$$\Delta G_{form} = [G(C_nO_m) - G(C)^*n - G(O)^*m] \,/\, (n+m), \quad (8)$$

where $G(C_nO_m)$ - Gibbs free energy C_nO_m compound, $G(C)$ and $G(O)$ - energies per atom of the most stable compounds consisting of pure carbon and pure oxygen, which are graphite and molecular oxygen, respectively. Then we plot ΔG_{form} as a function of composition $x = m/(n + m)$ and we find the convex hull of all these points. The points lying on the convex hull correspond to the thermodynamically stable phases, and the height above the convex hull (ΔG_h) indicates the decomposition energy of the given compound. At normal conditions (p = 1 atm and T = 300 K) the convex hull consists of only graphite, molecular oxygen and CO_2 gas.

In this study we use a simplified approach, in which we consider only individual C_nO_m molecules (neglecting the weak intermolecular van-der-Waals interactions). This allows us to estimate the value of the energies of formation without conducting complex predictions of the structures of the corresponding molecular crystals. Consequently, for the value of $G(C_nO_m)$ we took the Gibbs free energy of a single molecule C_nO_m. For pure carbon, instead of crystalline graphite, we take the largest magic carbon molecule considered here - C_{14} (this has the lowest energy per atom among carbon molecules studied here). For oxygen, we take the O_2 molecule in its triplet state. Calculated convex hull for all considered C_nO_m molecules is given in Fig. S2, ESI Section S1. Compounds lying on the convex hull are C_{14}, $C_{15}O_2$, $C_{15}O_9$, CO_2, O_2. In comparison with the conventional convex hull for the bulk C-O system, $C_{15}O_2$ and $C_{15}O_9$ appear on the convex hull. This is attributed to the energy difference between C_{14} molecule and graphite (the true stable bulk phase of carbon).

Finally, decomposition energy per mass is calculated as follows:

$$\Delta G_{release} = \Delta G_h^*(n+m) \;/\; M(C_nO_m). \quad (9)$$

The interpolated heatmap of $\Delta G_{release}$ is shown in Fig. 3b. One can see that $\Delta G_{release}$ follows the same pattern as in Fig. 3a, except small C_nO molecules ($n = 2$–8), which have quite high values of $\Delta G_{release}$. However,

these molecules are reactive and difficult to obtain. Molecules with O/C ratio significantly greater than 2 are also difficult to synthesize due to the instability of the peroxy O-O bonds. Thus, we confirm that the best candidates for HEDMs are molecular compositions between $1 \leq O/C \leq 2$ or near this range. Among such molecules we have identified magic ones which are the most promising compounds as HEDMs (they are marked by large asterisks on Fig. 3), as they can be synthesized more easily than others. Another area with relatively high $\Delta G_{release}$ (and ΔG_{frag}) is C_nO_3 and C_nO_4 molecules. However, among them, the only magic molecules are $C_{2n}O_4$ (n = 1–4), which contain 4-membered carbon rings. The height above the convex hull for 2,4,6-trinitrotoluene (4.203 MJ/kg) is close to the experimental value of its decomposition energy (4.190 MJ/kg), which indicates that our approximation works well.

This way we identified 32 high energy density C_nO_m molecules with caloricities comparable to those of well-known HEDMs, like TNT (2,4,6-trinitrotoluene). To do this we take the theoretical heat of explosion as $\Delta G_{release}$ and convert it into units used in practice (MJ/kg) from meV/a.m.u. used in quantum chemistry; C_nO_m molecules with $\Delta G_{release} > 2.5$ MJ/kg are presented in Table 1 (full data is given in Table S1, ESI, Section 1). For example, the theoretical heat of explosion for C_4O_9 is 3.4 MJ/kg, which is ~80 % of the heat of explosion of TNT (4.19 MJ/kg).

5. Conclusions

We have performed a systematic search for ground-state structures of all C_nO_m molecules in a wide compositional area ($0 \leq n, m \leq 16$) using the global optimization algorithm USPEX and DFT calculations. When considering which molecules are more likely to form, we applied the concept of "magicity" that proved fruitful in previous studies of nanoclusters and molecules. Such moleeules are the likeliest ones to appear in chemical reactions and to be found in nature (e.g. in the interstellar medium). We also investigated the fragmentation paths and energies of C_nO_m molecules. Based on general chemical thinking, the most favorable fragmentation channel involves the formation of the CO_2 molecule, which was confirmed by our calculations. Using the data obtained, we proposed a strategy to identify the most promising candidates as high energy density materials (HEDMs) by highlighting molecules that are likely to form (i.e. magic) and capable of releasing significant energy upon decomposition. The most interesting HEDMs are molecules in or near the range $1 \leq O/C \leq 2$, their thermal characteristics reaching up to 80 % of those of TNT. It is indeed surprising and inspiring how much can be discovered about such a seemingly well known system as C-O, with numerous carbon oxides finally understood within a unified picture where the concept of magicity explains the existence of the observed molecules.

CRediT authorship contribution statement

Elizaveta E. Vaneeva: Writing – review & editing, Writing – original draft, Validation, Methodology, Investigation, Formal analysis, Data curation, Conceptualization. **Sergey V. Lepeshkin:** Writing – review & editing, Writing – original draft, Supervision, Methodology, Formal analysis. **Dmitry V. Rybkovskiy:** Writing – review & editing, Formal analysis, Conceptualization. **Artem R. Oganov:** Writing – review & editing, Validation, Supervision, Conceptualization.

Declaration of competing interest

The authors declare that they have no known competing financial interests or personal relationships that could have appeared to influence the work reported in this paper.

Acknowledgements

This work was supported by the Russian Science Foundation (grant #19-72-30043). The calculations were performed on Oleg and Arkuda supercomputers at Skoltech and at the Joint Supercomputer Center of Russian Academy of Sciences, the Lobachevsky cluster at the University of Nizhny Novgorod and supercomputer "Govorun" at JINR. Authors would like to thank Pavel Butkaliuk for inspiring this work.

Appendix A. Supplementary data

Supplementary data to this article can be found online at https://doi.org/10.1016/j.mtener.2025.101821.

Data availability

All data is in the Supplementary file.

References

[1] R.I. Kaiser, A.M. Mebel, On the formation of higher carbon oxides in extreme environments, Chem. Phys. Lett. 465 (2008) 1–9, https://doi.org/10.1016/j.cplett.2008.07.076.
[2] R. Stimac, F. Kerek, H.-J. Apell, Macrocyclic carbon suboxide oligomers as potent inhibitors of the Na,K-ATPase, Ann. N. Y. Acad. Sci. 986 (2003) 327–329, https://doi.org/10.1111/j.1749-6632.2003.tb07204.x.
[3] S.K. Atreya, Z.G. Gu, Photochemistry and stability of the atmosphere of Mars, Adv. Space Res. 16 (1995) 57–68, https://doi.org/10.1016/0273-1177(95)00250-i.
[4] X. Hou, Y. Lu, Y. Ni, D. Zhang, Q. Zhao, J. Chen, Synthesis of a class of oxocarbons (C4O4, C5O5) and the application as high-capacity cathode materials for lithium-ion batteries, Sci. China Chem. 66 (2023) 2780–2784, https://doi.org/10.1007/s11426-023-1800-5.
[5] Y.L. Yung, W.B. DeMore, Photochemistry of Planetary Atmospheres, Oxford University Press, USA, 1999. https://books.google.com/books/about/Photochemistry_of_Planetary_Atmospheres.html?hl=&id=FY3mCwAAQBAJ.
[6] M. Salaris, I. Dominguez, E. Garcia-Berro, M. Hernanz, J. Isern, R. Mochkovitch, The cooling of CO white dwarfs: influence of the internal chemical distribution, Astrophys. J. 486 (1997) 413–419, https://doi.org/10.1086/304483.
[7] Y.-R. Luo, Comprehensive Handbook of Chemical Bond Energies, CRC Press, 2007. https://books.google.com/books/about/Comprehensive_Handbook_of_Chemical_Bond.html?hl=&id=kM3mwD4y_TAC.
[8] C. Mailhiot, L.H. Yang, A.K. McMahan, Polymeric nitrogen, Phys. Rev. B Condens. Matter 46 (1992) 14419–14435, https://doi.org/10.1103/physrevb.46.14419.
[9] M.I. Eremets, A.G. Gavriliuk, I.A. Trojan, D.A. Dzivenko, R. Boehler, Single-bonded cubic form of nitrogen, Nat. Mater. 3 (2004) 558–563, https://doi.org/10.1038/nmat1146.
[10] Y. Ma, A.R. Oganov, Z. Li, Y. Xie, J. Kotakoski, Novel high pressure structures of polymeric nitrogen, Phys. Rev. Lett. 102 (2009) 065501, https://doi.org/10.1103/PhysRevLett.102.065501.
[11] S. Yu, B. Huang, Q. Zeng, A.R. Oganov, L. Zhang, G. Frapper, Emergence of novel polynitrogen molecule-like species, covalent chains, and layers in magnesium–nitrogen mgxNy phases under high pressure, J. Phys. Chem. C Nanomater. Interfaces 121 (2017) 11037–11046, https://doi.org/10.1021/acs.jpcc.7b00474.
[12] S. Yu, Q. Zeng, A.R. Oganov, G. Frapper, B. Huang, H. Niu, L. Zhang, First-principles study of Zr–N crystalline phases: phase stability, electronic and mechanical properties, RSC Adv. 7 (2017) 4697–4703, https://doi.org/10.1039/c6ra27233a.
[13] S. Yu, Q. Zeng, A.R. Oganov, G. Frapper, L. Zhang, Phase stability, chemical bonding and mechanical properties of titanium nitrides: a first-principles study, Phys. Chem. Chem. Phys. 17 (2015) 11763–11769, https://doi.org/10.1039/c5cp00156k.
[14] J. Zhang, A.R. Oganov, X. Li, H. Niu, Pressure-stabilized hafnium nitrides and their properties, Phys. Rev. B Condens. Matter 95 (2017), https://doi.org/10.1103/physrevb.95.020103.
[15] X. Huang, F. Jiao, C. Zhang, Y. Chen, Y. Xie, W. Xie, Investigation of polymeric CO synthesized at high pressure and its stability under ambient conditions: a first-principles study, J. Phys. Chem. C Nanomater. Interfaces 126 (2022) 19571–19579, https://doi.org/10.1021/acs.jpcc.2c04467.
[16] C. Sun, W. Guo, J. Zhu, X. Li, Y. Yao, High-energy-density polymeric carbon oxide: layered CxOy solids under pressure, Phys. Rev. B Condens. Matter 104 (2021), https://doi.org/10.1103/physrevb.104.094102.
[17] B.C. Ferrari, C.J. Bennett, A computational investigation of the equilibrium geometries, energetics, vibrational frequencies, infrared intensities and Raman activities of C2Oy (y = 3, 4) species, Mol. Phys. 119 (2021) e1837404, https://doi.org/10.1080/00268976.2020.1837404.
[18] S. Evangelisti, Carbon-oxygen clusters as hypothetical high energy-density materials, Chem. Phys. 218 (1997) 21–30, https://doi.org/10.1016/s0301-0104(97)00005-0.
[19] A. Gambi, A.G. Giumanini, P. Strazzolini, Theoretical investigations on (CO)n (CO2)m cyclic cooligomers, THEOCHEM 536 (2001) 9–16, https://doi.org/10.1016/s0166-1280(00)00601-1.
[20] P. Strazzolini, A. Gambi, A.G. Giumanini, H. Vancik, The reaction between ethanedioyl (oxalyl) dihalides and Ag2C2O4: a route to Staudinger's elusive

ethanedioic (oxalic) acid anhydride, J. Chem. Soc. Perkin 1 (1998) 2553–2558, https://doi.org/10.1039/A803430C.
[21] Z. Song, Y. Qian, T. Zhang, M. Otani, H. Zhou, Poly(benzoquinonyl sulfide) as a high-energy organic cathode for rechargeable Li and Na batteries, Adv. Sci. 2 (2015) 1500124, https://doi.org/10.1002/advs.201500124.
[22] Website, (n.d.). [https://pubchem.ncbi.nlm.nih.gov/.
[23] A.R. Oganov, C.W. Glass, Crystal structure prediction using ab initio evolutionary techniques: principles and applications, J. Chem. Phys. 124 (2006) 244704, https://doi.org/10.1063/1.2210932.
[24] A.R. Oganov, A.O. Lyakhov, M. Valle, How evolutionary crystal structure prediction works–and why, Acc. Chem. Res. 44 (2011) 227–237, https://doi.org/10.1021/ar1001318.
[25] S.V. Lepeshkin, V.S. Baturin, Y.A. Uspenskii, A.R. Oganov, Method for simultaneous prediction of atomic structure and stability of nanoclusters in a wide area of compositions, J. Phys. Chem. Lett. 10 (2019) 102–106, https://doi.org/10.1021/acs.jpclett.8b03510.
[26] G. Kresse, J. Furthmüller, Efficient iterative schemes for ab initio total-energy calculations using a plane-wave basis set, Phys. Rev. B Condens. Matter 54 (1996) 11169–11186, https://doi.org/10.1103/physrevb.54.11169.
[27] G. Kresse, J. Hafner, Ab initio molecular dynamics for liquid metals, Phys. Rev. B Condens. Matter 47 (1993) 558–561, https://doi.org/10.1103/physrevb.47.558.
[28] P.E. Blöchl, Projector augmented-wave method, Phys. Rev. B Condens. Matter 50 (1994) 17953–17979, https://doi.org/10.1103/physrevb.50.17953.
[29] J.P. Perdew, K. Burke, M. Ernzerhof, Generalized gradient approximation made simple, Phys. Rev. Lett. 77 (1996) 3865–3868, https://doi.org/10.1103/PhysRevLett.77.3865.
[30] P.J. Stephens, F.J. Devlin, C.F. Chabalowski, M.J. Frisch, Ab initio calculation of vibrational absorption and circular dichroism spectra using density functional force fields, J. Phys. Chem. 98 (1994) 11623–11627, https://doi.org/10.1021/j100096a001.
[31] S.V. Lepeshkin, V.S. Baturin, A.S. Naumova, A.R. Oganov, "Magic" molecules and a new look at chemical diversity of hydrocarbons, J. Phys. Chem. Lett. 13 (2022) 7600–7606, https://doi.org/10.1021/acs.jpclett.2c02098.
[32] E.E. Vaneeva, S.V. Lepeshkin, A.R. Oganov, Prediction and rationalization of abundant C-N-H molecules in different environments, J. Phys. Chem. Lett. 14 (2023) 8367–8375, https://doi.org/10.1021/acs.jpclett.3c01753.
[33] D.S. Sabirov, I.S. Shepelevich, Information entropy of oxygen allotropes. A still open discussion about the closed form of ozone, Comput. Theor. Chem. 1073 (2015) 61–66, https://doi.org/10.1016/j.comptc.2015.09.016.
[34] D.V. Rybkovskiy, S.V. Lepeshkin, A.A. Mikhailova, V.S. Baturin, A.R. Oganov, Lithiation of phosphorus at the nanoscale: a computational study of LiP clusters, Nanoscale 16 (2024) 1197–1205, https://doi.org/10.1039/d3nr05166h.
[35] A.A. Mikhailova, S.V. Lepeshkin, V.S. Baturin, A.P. Maltsev, Y.A. Uspenskii, A. R. Oganov, Ultralow reaction barriers for CO oxidation in Cu-Au nanoclusters, Nanoscale 15 (2023) 13699–13707, https://doi.org/10.1039/d3nr02044d.
[36] M. Fedyaeva, S. Lepeshkin, A.R. Oganov, Stability of sulfur molecules and insights into sulfur allotropy, Phys. Chem. Chem. Phys. 25 (2023) 9294–9299, https://doi.org/10.1039/d2cp05498a.
[37] D.V. Rybkovskiy, S.V. Lepeshkin, V.S. Baturin, A.A. Mikhailova, A.R. Oganov, Phosphorus nanoclusters and insight into the formation of phosphorus allotropes, Nanoscale 15 (2023) 1338–1346, https://doi.org/10.1039/d2nr06523a.
[38] H.J. Novinsky, R. Pflaum, P. Pfau, K. Sattler, E. Recknagel, Mass spectrometric studies on lead compound clusters, Surf. Sci. 156 (1985) 126–133, https://doi.org/10.1016/0039-6028(85)90565-5.
[39] X. Xing, Z. Tian, H. Liu, Z. Tang, Magic bimetallic cluster anions of M/Pb (M = Au, Ag and Cu) observed and analyzed by laser ablation and time-of-flight mass spectrometry, Rapid Commun. Mass Spectrom. 17 (2003) 1411–1415, https://doi.org/10.1002/rcm.1063.
[40] T.W. Yen, S.K. Lai, Use of density functional theory method to calculate structures of neutral carbon clusters Cn ($3 \leq n \leq 24$) and study their variability of structural forms, J. Chem. Phys. 142 (2015) 084313, https://doi.org/10.1063/1.4908561.
[41] G. Maier, H.P. Reisenauer, U. Schäfer, H. Balli, C5O2 (1,2,3,4-pentatetraene-1,5-dione), a new oxide of carbon, Angew Chem. Int. Ed. Engl. 27 (1988) 566–568, https://doi.org/10.1002/anie.198805661.
[42] Y. Vallee, Gas Phase Reactions in Organic Synthesis, CRC Press, 1998. https://play.google.com/store/books/details?id=lfBC9hj9iH8C.
[43] M. Ohishi, H. Suzuki, S.-I. Ishikawa, C. Yamada, H. Kanamori, W.M. Irvine, R. D. Brown, P.D. Godfrey, N. Kaifu, Detection of a new carbon-chain molecule, CCO, Astrophys. J. 380 (1991) L39–L42, https://doi.org/10.1086/186168.
[44] H.E. Matthews, W.M. Irvine, P. Friberg, R.D. Brown, P.D. Godfrey, A new interstellar molecule: tricarbon monoxide, Nature 310 (1984) 125–126, https://doi.org/10.1038/310125a0.
[45] F. Wöhler, Ueber die honigsteinsäure, Ann. Phys. 83 (1826) 325–334, https://doi.org/10.1002/andp.18260830706.
[46] H. Meyer, K. Steiner, Über ein neues Kohlenoxyd C 12 O 9, Ber. Dtsch. Chem. Ges. 46 (1913) 813–815, https://doi.org/10.1002/cber.191304601105.
[47] X. Bao, X. Zhou, C. Flener Lovitt, A. Venkatraman, D.A. Hrovat, R. Gleiter, R. Hoffmann, W.T. Borden, Molecular orbitals of the oxocarbons (CO)n, n = 2-6. Why does (CO)4 have a triplet ground state? J. Am. Chem. Soc. 134 (2012) 10259–10270, https://doi.org/10.1021/ja3034087.
[48] B.I. Dunlap, I.V. Schweigert, A.P. Purdy, A.W. Snow, A. Hu, Thermodynamic and kinetic stabilities of CO2 oligomers, J. Chem. Phys. 138 (2013) 134304, https://doi.org/10.1063/1.4797465.
[49] M.J. Rodig, A.W. Snow, P. Scholl, S. Rea, Synthesis and low temperature spectroscopic observation of 1,3,5-trioxane-2,4,6-trione: the cyclic trimer of carbon dioxide, J. Org. Chem. 81 (2016) 5354–5361, https://doi.org/10.1021/acs.joc.6b00647.
[50] C.S. Jamieson, A.M. Mebel, R.I. Kaiser, First detection of the C2 symmetric isomer of carbon pentaoxide (CO5) at 10K, Chem. Phys. Lett. 443 (2007) 49–54, https://doi.org/10.1016/j.cplett.2007.06.009.
[51] C.S. Jamieson, A.M. Mebel, R.I. Kaiser, First detection of the Cs symmetric isomer of carbon hexaoxide (CO6) at 10K, Chem. Phys. Lett. 450 (2008) 312–317, https://doi.org/10.1016/j.cplett.2007.11.052.